Journal of Applied Polymer Science

Effect of amphiphilic compatibilizers on the filler dispersion and properties of polyethylene—thermally reduced graphene nanocomposites

Vikas Mittal, Ali U. Chaudhry*
Department of Chemical Engineering, The Petroleum Institute, Abu Dhabi, UAE
*Present address: Metallurgical & Materials Engineering, Colorado School of Mines, Golden Colorado, USA
Correspondence to: V. Mittal (E-mail: vmittal@pi.ac.ae)

ABSTRACT: Compatibilizers of different chemical structures and specifications were used to enhance the filler exfoliation in nanocomposites of polyethylene and thermally reduced graphene prepared by melt mixing route. The mechanical performance of the compatibilized nanocomposites was observed to be better than PE/G nanocomposites due to enhanced extent of filler exfoliation and distribution. Highest increase of 45% in tensile modulus and 13% in peak stress was observed in the composites. Overall, from the mechanical, rheological, thermal, and calorimetric properties, the compatibilizers with best performance were ethylene acrylic acid (EAA) copolymer and chlorinated polyethylene (CPE25). Furthermore, the extent of filler exfoliation was observed to increase with increasing EAA content thus confirming positive interactions between EAA and thermally reduced graphene, though no specific chemical interactions could be detected. The composite properties were observed to reach maximum around 7.5 wt % EAA content, followed by reduced performance due to extensive matrix plasticization. The observed behaviors were a result of interplay of opposing factors like filler exfoliation due to compatibilizer addition and matrix plasticization due to its lower molecular weight, thus the observed optimum comaptibilizer amount was specific to the compatibilizer. © 2015 Wiley Periodicals, Inc. J. Appl. Polym. Sci. **2015**, *132*, 42484.

KEYWORDS: composites; morphology; properties and characterization

Received 22 February 2015; accepted 10 May 2015
DOI: 10.1002/app.42484

INTRODUCTION

Graphene consists of one atomic thick sheet of covalently sp^2-bonded carbon atoms in a hexagonal arrangement. A single defect-free graphene layer has been estimated to have Young's modulus of ≈1.0 TPa, intrinsic strength ≈42 N/m, thermal conductivity ≈4840–5300 W/(m.K), electron mobility exceeding 25,000 cm^2/V.s, excellent gas impermeability, and specific surface area of ≈2630 m^2/g.[1] Though these properties represent the characteristics of defect-free materials, and generating defect-free materials is cumbersome, however, the average properties of graphene-based materials even with some degree of surface and structural defects are still promising. As a result of its superior reinforcement potential, a number of studies on polymer nanocomposites based on graphene have been reported in the recent years.[1–9]

Thermodynamic factors such as interfacial compatibility of polymer and filler phases as well as kinetic factors such as filler shape and size, dispersion techniques and equipment, time of mixing, and applied shear lead to final morphology in the polymer nanocomposites.[10–15] In the case of graphene, the presence of less number of functional groups (such as carboxyl, epoxide, and hydroxyl) on the surface of its platelets leads to lower compatibility with polar polymer matrices, thus resulting in poor dispersion and lower enhancement in polymer properties.[1] Similarly, the dispersion of polar graphene oxide in nonpolar polymers like polyethylene is not optimal owing to absence of positive interactions between them.

One of the routes to modify/tune the surface characteristics of graphene platelets to enhance their dispersion potential in polymer matrices is the functionalization of their surface, which results in significant enhancement of the mechanical and electrical properties in polymer nanocomposites. For instance, Ramanathan *et al.* prepared nanocomposites of poly(methyl methacrylate) (PMMA) and partially oxygenated functionalized sheets of expanded graphene by sonication and high-speed shearing,[16] which resulted in superior thermal performance as compared to single-walled carbon nanotubes (SWCNTs) and expanded graphite platelets. Ansari and Giannelis incorporated functionalized graphene sheets in a PVDF matrix by solution mixing and melt blending which resulted in percolation at a much lower filler amount.[17] Castelain *et al.* reported different

chemical routes to functionalize graphene with short-chain polyethylene, which influenced the mechanical properties of graphene-based high-density polyethylene (HDPE) nanocomposites.[18] In another study, Wang *et al.* prepared low-density polyethylene (LDPE)/graphene nanocomposites using vinyl functionalized graphene sheets and LDPE through solution blending method.[19] Similarly, Yun *et al.* also studied the reinforcing effect of alkylated graphene oxide (AGO) on a nonpolar polypropylene matrix.[20]

The other method described in literature is the addition of amphiphilic compatibilizer, which does not require any additional step of functionalization of filler surface. In case of polyethylene, the lack of polar groups in its backbone is a considerable hurdle in homogenous dispersion and exfoliation of nanofillers. Introduction of amphiphilic compatibilizer having polar and nonpolar groups acting as bridges between filler and host polymer results in improved filler dispersion. Osman *et al.* reported that introduction of a block copolymer-based polyethylene-block-polyethylene glycol (PE-*b*-PEG) compatibilizer in HDPE and clay nanocomposite improved exfoliation of clay particles, which resulted in superior mechanical and oxygen permeation properties.[21] Similarly, Schniepp *et al.* used maleic anhydride as a bridge for nanocomposites of LDPE and exfoliated graphite nanoplatelets.[22] Chaudhry and Mittal[23] in a previous study reported the advantage of introducing different extents of chlorinated polyethylene copolymers of varying chlorination level on HDPE–graphene nanocomposites. Both mechanical and rheological properties were enhanced with higher extent of filler exfoliation achieved for comaptibilizer with higher chlorination level in the structure. Similarly, Vasileiou *et al.*[24] reported the dispersion and properties of polyethylene–graphene composite using maleated linear low-density polyethylene (LLDPE) derivatives and thermally reduced graphene oxide (TRG) through a noncovalent compatibilization approach. Yu *et al.*[25] prepared a flame retardant functionalized GO (FRs-FGO) using amine functional GO and phosphoramide oligomer, which was incorporated into PP and simultaneously compatibilized with PP-grafted maleic anhydride (PP-g-MA). In an interesting study, Seo *et al.*[26] also reported the compatibility of functionalized graphene with polyethylene (PE) as well as its copolymers as a function of molecular weight and polarity.

Though different compatibilizers have been reported in the literature to enhance graphene dispersion in the nonpolar polymer matrices, but the use of various graphene types with different C/O ratios, different surface modifications and polymer grades as well as different synthesis routes to generate nanocomposites makes the comparison of the resulting nanocomposite properties difficult. Moreover, a systematic study using a wide variety of compatibilizers with different functionalities is required in order to generate insights on potential compatibilizers, while keeping the filler type and nanocomposite generation route constant. Thus, the goal of the current study was to explore the effect of a variety of different compatibilizers on the mechanical, rheological, thermal, and morphological characteristics of nanocomposites generated by melt mixing with HDPE as matrix and thermally reduced graphene (of low polarity) as filler. The amount of the composite constituents was held constant in order to correlate the observed property changes to the specific compatibilizer and its interactions with the filler surface as well as matrix polymer. Comparisons of properties of nanocomposites with those generated with commonly used layered silicate clay minerals have been demonstrated to confirm the potential of graphene as high-potential reinforcing filler in the presence of compatibilizer.

Table I. Compatibilizers Used for the Study and the Corresponding Composite Codes

Compatibilizer name	Composite code
–	PE/G
Ethylene acrylic acid copolymer	PE/G/EAA
Ethylene vinyl acetate-g-maleic anhydride	PE/G/EVA-MA
Enhanced polyethylene resin	PE/G/EPE
Ethylene methyl acrylate copolymer	PE/G/EMA1
Ethylene methyl acrylate copolymer	PE/G/EMA2
Ethylene methacrylic acid copolymer with zinc ion	PE/G/EMAZ
Ethylene-α-olefin copolymer	PE/G/E-AO
Chlorinated polyethylene 25%	PE/G/CPE25
Chlorinated polyethylene 35%	PE/G/CPE35
Ethylene butyl acrylate copolymer	PE/G/EBA
Ethylene-g-maleic anhydride copolymer	PE/G/PE-MA

EXPERIMENTAL

Materials

HDPE (BB2581) of specific gravity 0.958 was supplied by Abu Dhabi Polymers Company Limited (Borouge), UAE. Various copolymer-based compatibilizers of different specifications and functionalities were procured from suppliers as mentioned in Tables I and II. The polymer materials were used as obtained. Thermally reduced graphene was prepared through thermal exfoliation of precursor graphite oxide[27] using modified Hummer's method,[28] as reported earlier[23]. Graphene was generated via thermal exfoliation of graphite oxide by placing 1 g in a long quartz tube with 25 mm internal diameter and sealed at one end. The sample was flushed with nitrogen, followed by insertion of the tube in a tube furnace preheated to 1050°C. The tube was held in the furnace for 30 s.

Preparation of Nanocomposites

The nanocomposites were prepared by melt mixing of polymer and compatibilizers with thermally reduced graphene using a mini twin screw extruder (MiniLab HAAKE Rheomex CTW5, Germany). The screw length and screw diameter were 109.5 mm and 5/14 mm conical, respectively. Batch size of 5 g was used and the shear mixing was performed for 5 min at 60 rpm. Compounding temperature of 190°C was maintained for all the nanocomposites. Pure polymer as well as nanocomposite without compatibilizers was also processed by subjecting them to similar shear and thermal conditions. The amount of compatibilizers was 5 wt %, whereas graphene content in the nanocomposites was fixed at 1 wt %. Disc and dumbbell shaped

Table II. Specifications of HDPE and Compatibilizers as Obtained from Suppliers

Polymer/ compatibilizer	Supplier and trade name	Co-monomer content (%)	MFI, g/10 min (2.16 kg, 190°C)	Density (g/cm^3)	Peak melting temperature (°C)
PE	Borouge BB2581	–	0.35	0.958	147
EAA	Exxon Mobil ESCOR 5050	9% AA	8.4	0.936	97
EVA-MA	Dupont Fusabond C190	–	16	0.950	71
EPE	Dow ELITE 5230F	–	4	0.916	122
EMA1	Dupont Elvaloy AC 12024S	24% MA	20	0.944	88
EMA2	Dupont Elvaloy AC 15024S	24% MA	50	0.944	88
EMAZ	Dupont Surlyn 9020	–	1	0.96	85
E-AO	Dow Affinity EG8150G	–	0.5	0.868	56
CPE25	Lianda Corporation, Weipren 6025	25% Chlorination	1.8	1.1–1.3	140
CPE35	Xuran Chemicals	35% Chlorination	1.9	1.1–1.16	Amorphous
EBA	Dupont Elvaloy AC34035	35% BA	40	0.93	90
PE-MA	Aldrich PE-g-MA	–	500 cP viscosity (140°C)	–	–

test specimens were injection molded using a mini injection molding machine (HAAKE MiniJet, Germany), applying same processing temperatures as used during compounding. The injection pressure was 700 bars for 6 s, whereas holding pressure was 400 bars for 3 s. The temperature of the mold was kept at 50°C.

Characterization of Nanocomposites

Tensile testing of nanocomposites was carried out on universal testing machine from Testometric, UK. Dumbbell-shaped samples of dimensions: length 73 mm, gauge length 30 mm, width 4 mm, and thickness 2 mm were used. A loading rate of 4 mm/min was used and the tests were carried out at room temperature. Tensile modulus and yield stress were calculated using built in software Win Test Analysis and an average of five values was reported.

Rheological properties of the nanocomposites were measured using AR 2000 Rheometer from TA Instruments at 190°C. Disc-shaped samples of diameter 25 mm and thickness 2 mm were used and a gap opening of 1.6 mm was fixed during the test. Strain sweeps were recorded at $\omega = 1$ rad/s from 0.1 to 100% strain and the nanocomposites were observed to be stable up to 10% strain. Frequency sweeps (dynamic testing) were, thus, recorded at 4% strain from $\omega = 0.1$ to 100 rad/s.[29]

Perkin-Elmer Pyris-1 differential scanning calorimeter (DSC) was used to measure the calorimetric properties of nanocomposites under nitrogen atmosphere. The scans were obtained from 50–200–50°C using heating and cooling rates of 15°C/min and 5°C/min, respectively. The heat enthalpies were measured with an error of ±0.1% and were confirmed by repeating the runs. Netzsch thermogravimetric analyzer (TGA) was used to record the thermal degradation properties of nanocomposites. Nitrogen was used as a carrier gas and the scans were obtained from 50°C to 700°C using a heating rate of 20°C/min.

The microstructure of the nanocomposites was analyzed using scanning electron microscope (FEI Quanta, FEG250, USA) at accelerating voltages of 10–20 kV. The sample surfaces were sputter coated with 3 nm thick gold layer. Transmission electron microscopy (TEM) of nanocomposite samples was performed using EM 912 Omega (Zeiss, Oberkochen BRD) electron microscope at 120 kV and 200 kV accelerating voltage. Thin sections of 70–90 nm thickness were microtomed from the block of the specimen and were subsequently supported on 100 mesh grids sputter coated with a 3 nm thick carbon layer.

RESULTS AND DISCUSSION

The energy-dispersive X-ray (EDX) analysis of thermally reduced graphene used for the study exhibited a C/O ratio of 22, thus indicating moderate polarity of the platelets' surface. The thermally reduced graphene, reported in an earlier study, with C/O ratio of 20 had presence of polar surface groups (hydroxyl, epoxide, carboxyl, etc.). Thus, these functional groups present on the filler surface can be expected to physically or chemically interact with the polar compatibilizers used in the study leading to filler delamination in nonpolar PE. The choice of the compatibilizers was made on the basis of functional groups and their amount in the copolymers. The nonpolar component of the compatibilizers was based on polyethylene in order to attain compatibility with the matrix polymer. For instance, as mentioned in Table II, ethylene acrylic acid (EAA) copolymer had 9% acrylic acid content in its structure, whereas the rest was PE. Ethylene methyl acrylate copolymers EMA1 and EMA2 had 24% methyl acrylate content, but different melt flow indices in order to analyze the impact of molecular weight of compatibilizers. Similarly, ethylene butyl acrylate copolymer EBA with 35% butyl acrylate content was used in order to study the effect of different acrylates as well as their content. Chlorinated polyethylene compatibilizers CPE25 and CPE35 had 25% and 35% chlorination levels on PE backbone. The interactions of maleic anhydride with the filler surface were studied through ethylene vinyl acetate-g-maleic anhydride (EVA-MA) and polyethylene-g-maleic anhydride (PE-MA) compatibilizers.

Table III. Tensile Properties of Nanocomposites with Various Compatibilizers (Graphene Content: 1 wt %, Compatibilizer Content: 5 wt %)

Composite	Tensile modulus[a] (MPa)	Yield strain[b] (%)	Peak stress[c] (Mpa)	Total elongation[d] (mm)
PE	1063	9.0	62	4.4
PE/G	1203	8.5	61	4.0
PE/G/EAA	1489	8.5	70	4.6
PE/G/EVA-MA	1067	8.2	57	4.4
PE/G/EPE	1370	8.4	70	4.5
PE/G/EMA1	1222	8.3	51	4.7
PE/G/EMA2	1412	8.3	66	4.4
PE/G/EMAZ	1327	8.9	60	4.7
PE/G/E-AO	1546	8.5	64	4.6
PE/G/CPE25	1557	7.6	68	4.1
PE/G/CPE35	1268	8.5	64	4.4
PE/G/EBA	1420	7.9	64	4.5
PE/G/PE-MA	1234	8.4	69	4.5

[a] Relative probable error 5%.
[b] Relative probable error 5%.
[c] Relative probable error 15%.
[d] Relative probable error 15%.

Enhanced polyethylene (EPE) ethylene-α-olefin (E-AO) copolymers were plastomers with high impact strength and elasticity to reduce the strain hardening of the polymer on filler addition. Ionomer ethylene methacrylic acid copolymer with zinc ion (EMAZ) was used to study the effect of ionic species in generating ionic interactions with the filler surface. The melt flow indices of the compatibilizers varied between 0.5 and 50, thus indicating a wide variation of their molecular weight characteristics. For nanocomposite generation, the compounding conditions as well as the amounts of composite constituents were held constant in order to attribute the observed properties solely to compatibilizers and their interactions with filler surface. Subsequently, composites with varying amount of EAA comaptibilizer were also generated in order to study the effect of compatibilizer content on the nanocomposite properties.

Table III demonstrates the tensile properties of the nanocomposites. The tensile modulus of pure polymer was measured to be 1063 MPa, which was enhanced by 13% to 1203 MPa for PE/G nanocomposites. In most of the compatibilized nanocomposites, the tensile modulus was higher than PE/G nanocomposite, indicating that the compatibilizer resulted in improved filler distribution in PE matrix which led to better tensile modulus. Different extents of modulus enhancements also revealed different degrees of interactions between the filler and compatibilizers. Highest increment in modulus in the range of 40–45% was observed for CPE25, E-AO, and EAA compatibilizers. EBA and EMA2 also exhibited nearly 35% increment in the modulus as compared to pure polymer. EMA1, on the other hand, did not show any improvement as compared to PE/G composite, indicating that the lower MFI may not have resulted in better mixing with filler during compounding. CPE35 was reported earlier to enhance filler exfoliation as compared to CPE25, but its overall increment in modulus was only 20% due to its amorphous nature which led to extensive matrix plasticization.[23] Poorest response was observed from EVA-MA compatibilizer, probably due to its very high polarity which made it incompatible with matrix polymer. The other comaptibilizer PE-MA with maleic anhydride content also had a modest enhancement of 15% in the modulus, thus confirming that the MA containing compatibilizers did not interact well with the filler surface. The yield strain in the nanocomposites with E-AO and EAA compatibilizers also remained fairly close to PE, whereas a significant reduction was observed for CPE25 compatibilizer indicating strain hardening of the chains. CPE25 was earlier reported to be semi-crystalline compatibilizer with high melting point, which would have resulted in the observed reduction in yield strain.[23] Similar to tensile modulus, EAA and CPE25 comaptibilizer also exhibited one of the highest peak stress values along with other compatibilizers like EPE and PE-MA. However, it has to be noted that the relative probable error for peak stress measurements was 15%, as compared to 5% for modulus. CPE25 incorporation resulted in reduction in overall elongation, which was observed to increase as compared to PE for EAA, EMA1, EMAZ, and E-AO compatibilizers.

Figure 1 demonstrates the storage modulus of the nanocomposites as a function of angular frequency. The nanocomposites exhibited higher storage modulus than matrix polymer for the whole measurement range, though the differences diminished at higher angular frequencies. PE/G/EAA nanocomposite showed the highest magnitude of storage modulus. For instance, the G′ value for pure PE at 1 rad/s was 14,600 Pa, which was measured to be 45,340 Pa for PE/G/EAA nanocomposites and was even higher than 39,690 Pa for PE/G nanocomposite. All other compatibilized nanocomposites exhibited lower storage modulus than PE/G. Similar to tensile properties, EMA2 had better rheological performance than EMA1 and its higher MFI did not negatively impact the modulus probably due to higher extent of filler exfoliation. It was also observed that the nanocomposites PE/G/EVA-MA and PE/G/PE-MA though had poor tensile modulus, but exhibited high storage modulus values probably due to filler aggregates which resulted in higher shear resistance, as earlier observed for poly-L-lactide composites.[30] Transition point from liquid-like to solid-like viscoelastic behavior (gel point), where the polymer acts as true viscoelastic fluid due to lesser molecular flexibility and mobility, was observed at a frequency of 2.5 rad/s for PE/G composite. For PE/G/EAA nanocomposite, such transition was observed around 2 rad/s, indicating that the addition of 5 wt % of EAA compatibilizer did not lead to viscous domination due to matrix plasticization or this effect was overcome by the enhanced extent of filler exfoliation (Figure 1c). The PE/G/CPE25 and PE/G/E-AO nanocomposites exhibited these transitions at 5 and 10 rad/s frequencies, indicating more viscous response due to these compatibilizers. As shown in Figure 2, the complex viscosity of the nanocomposites also exhibited similar trends as storage modulus. Though PE/G/EAA exhibited highest magnitude of viscosity, it did not pose any difficulty during compounding and subsequent processing operations. The transition between viscosity and elasticity was also

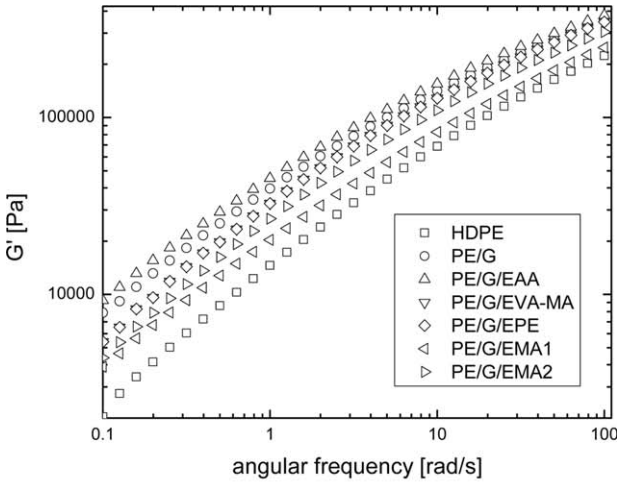

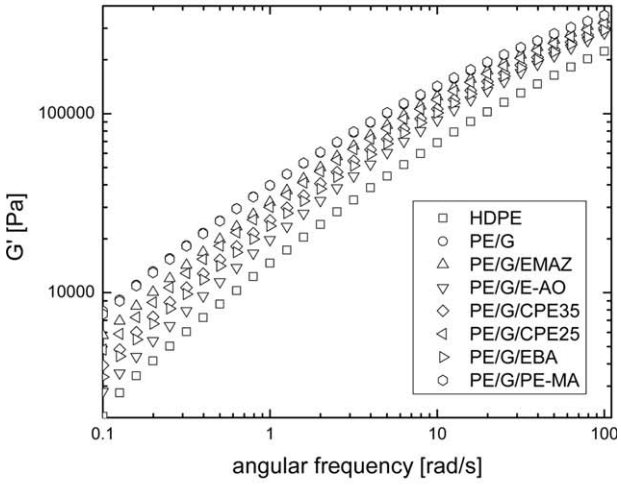

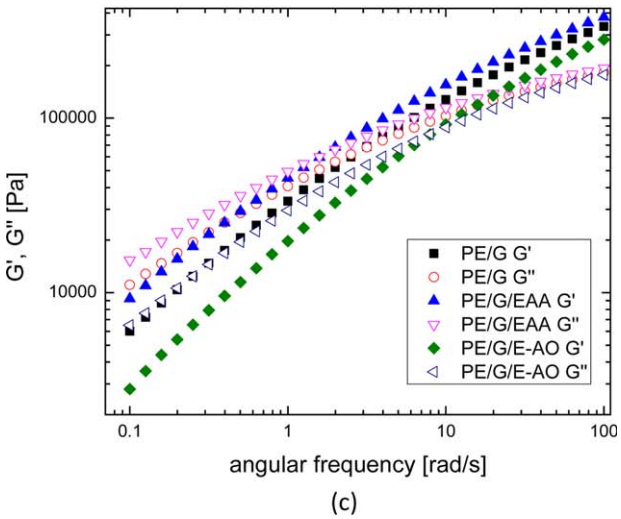

Figure 1. (a) and (b) Storage modulus of the nanocomposites as a function of angular frequency compared with pure polymer; (c) transition point of PE/G, PE/G/EAA, and PE/G/E-AO nanocomposites. [Color figure can be viewed in the online issue, which is available at wileyonlinelibrary.com.]

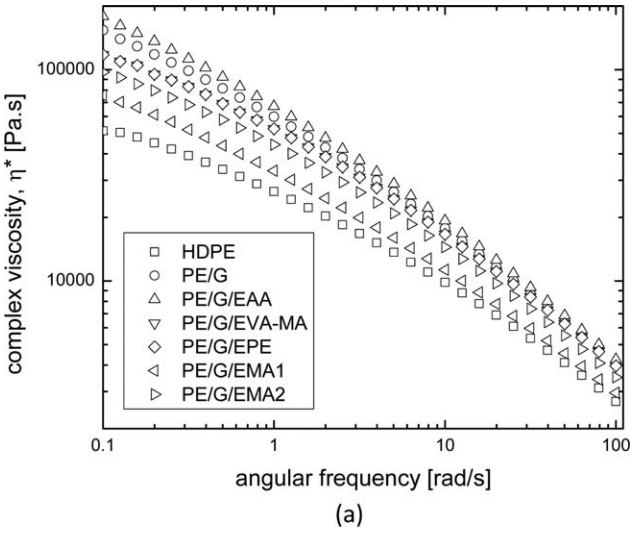

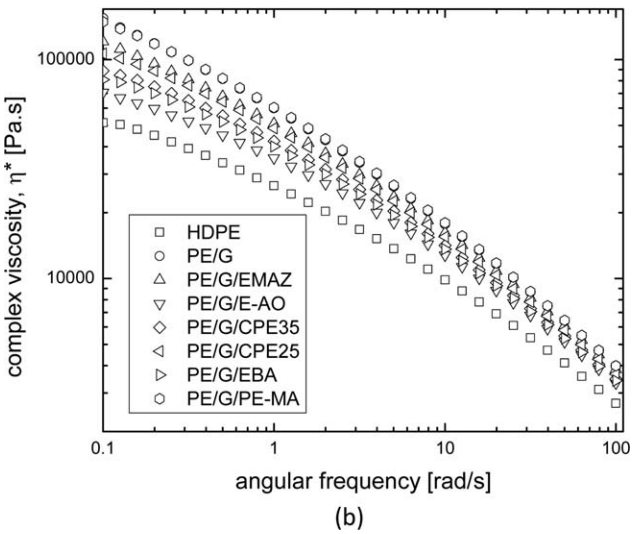

Figure 2. (a) and (b) Complex viscosity of the nanocomposites as a function of angular frequency compared with pure polymer.

observed at similar frequencies as storage and loss modulus. It has to be noted that the observed changes in the rheological and mechanical properties of nanocomposites resulted from synergistic combination of factors like possible matrix plasticization due to comaptibilizer addition thus reducing the properties and enhanced filler exfoliation due to better filler-polymer compatibility thus enhancing the properties.[23,31] These behaviors are, thus, strongly dependent on the amounts of filler and compatibilizer in the composite.

The thermal degradation performance of the nanocomposites is shown in Figure 3. A gradual increase in the onset and peak thermal degradation temperatures in nanocomposites as compared to pure PE was observed and compatibilized nanocomposites were even more stable than the PE/G nanocomposite. It indicated that the addition of 5 wt % of low molecular weight amphiphilic compatibilizers in the presence of graphene did not adversely affect the thermal properties of the matrix. The increment in the degradation temperatures in nanocomposites also

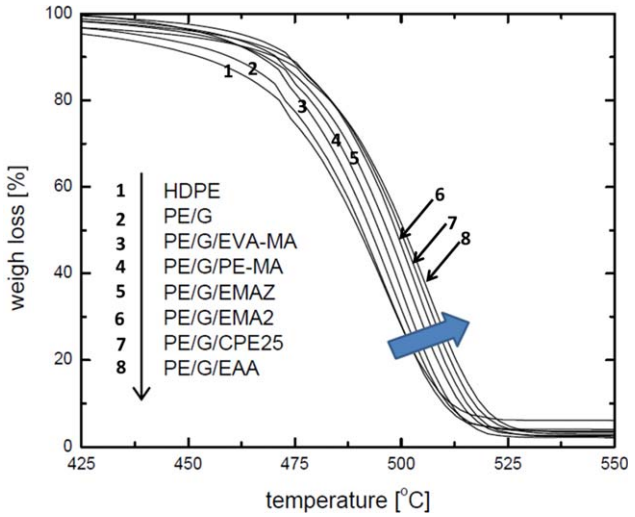

Figure 3. Cumulative thermograms demonstrating the thermogravimetric analysis of nanocomposites. [Color figure can be viewed in the online issue, which is available at wileyonlinelibrary.com.]

followed the trends in tensile properties. As the improvement in tensile properties was attributed to better filler exfoliation and corresponding stress transfer from polymer chains to graphene platelets, such delamination of filler in the polymer matrix thus also resulted in better heat transfer from the polymer phase to filler platelets. PE/G/EAA was the most thermally stable nanocomposite, with an approximate enhancement of 10°C in both onset and peak degradation temperatures as compared to matrix PE. Table IV and Figure 4 also describe the calorimetric properties of the nanocomposites. The melt enthalpy of 151 J/g in pure PE was reduced to 146 J/g in PE/G nanocomposite, indicating reduction in crystallinity by addition of graphene. Incorporation of CPE25 increased the melt enthalpy to 153 J/g due to its semi-crystalline nature, which also resulted in its decreased yield strain. Other compatibilizers reduced the melt

Table IV. Calorimetric Properties of Nanocomposites with Various Compatibilizers (Graphene Content: 1 wt %, Compatibilizer Content: 5 wt %)

Composite	ΔH (J/g)	Peak meting point (°C)	Peak crystallization point (°C)	Crystallinity (%)
PE	151	135.9	115.5	52
PE/G	146	135.8	115.0	50
PE/G/EAA	148	137.8	115.3	51
PE/G/EVA-MA	139	139.6	114.7	48
PE/G/EPE	138	137.4	114.9	48
PE/G/EMA1	147	137.3	115.0	51
PE/G/EMA2	128	137.1	115.4	44
PE/G/EMAZ	121	134.3	115.6	42
PE/G/E-AO	145	137.3	115.6	50
PE/G/CPE25	153	138.1	115.4	52
PE/G/CPE35	144	133.0	116.1	50
PE/G/EBA	121	138.6	115.5	42
PE/G/PE-MA	145	140.0	114.4	50

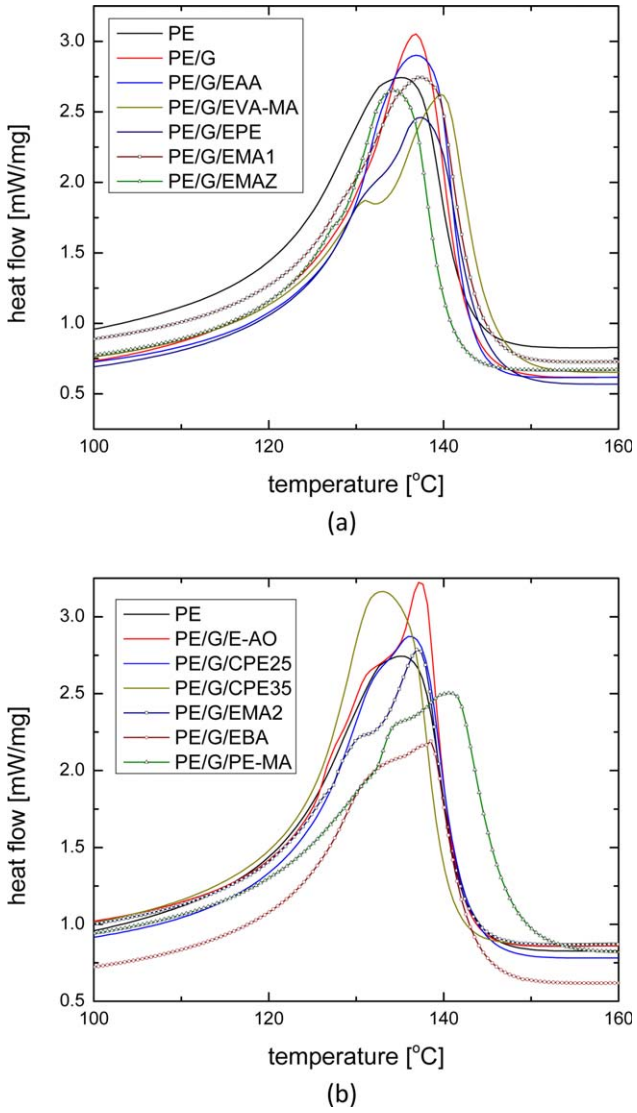

Figure 4. (a) and (b) DSC thermograms of nanocomposites with and without compatibilizers in comparison with the pure polymer. [Color figure can be viewed in the online issue, which is available at wileyonlinelibrary.com.]

enthalpy in the range of 138–145 J/g, leading to relative crystallinity in the range of 48–51%. EMAZ, EBA, and EMA2 exhibited significantly reduced enthalpy in the range of 121–128 J/g and the DSC thermograms of these components had dual peaks indicating possible incompatibility with matrix phase. Other compatibilizers PE-MA, E-AO, EVA-MA, and EPE also exhibited dual peaks in the DSC thermograms probably due to lack of miscibility at molecular level. The compatibilizers did not affect the crystallization of polymer as onset and peak crystallization temperatures were in the range of ±1°C of pure polymer. From the mechanical, rheological, and thermal performance of the nanocomposites, it was obvious that EAA, CPE25, and E-AO compatibilizers had highest impact on the nanocomposite performance.

Figure 5 shows the SEM micrographs of pristine graphene platelets as well as their state of dispersion in nanocomposites with

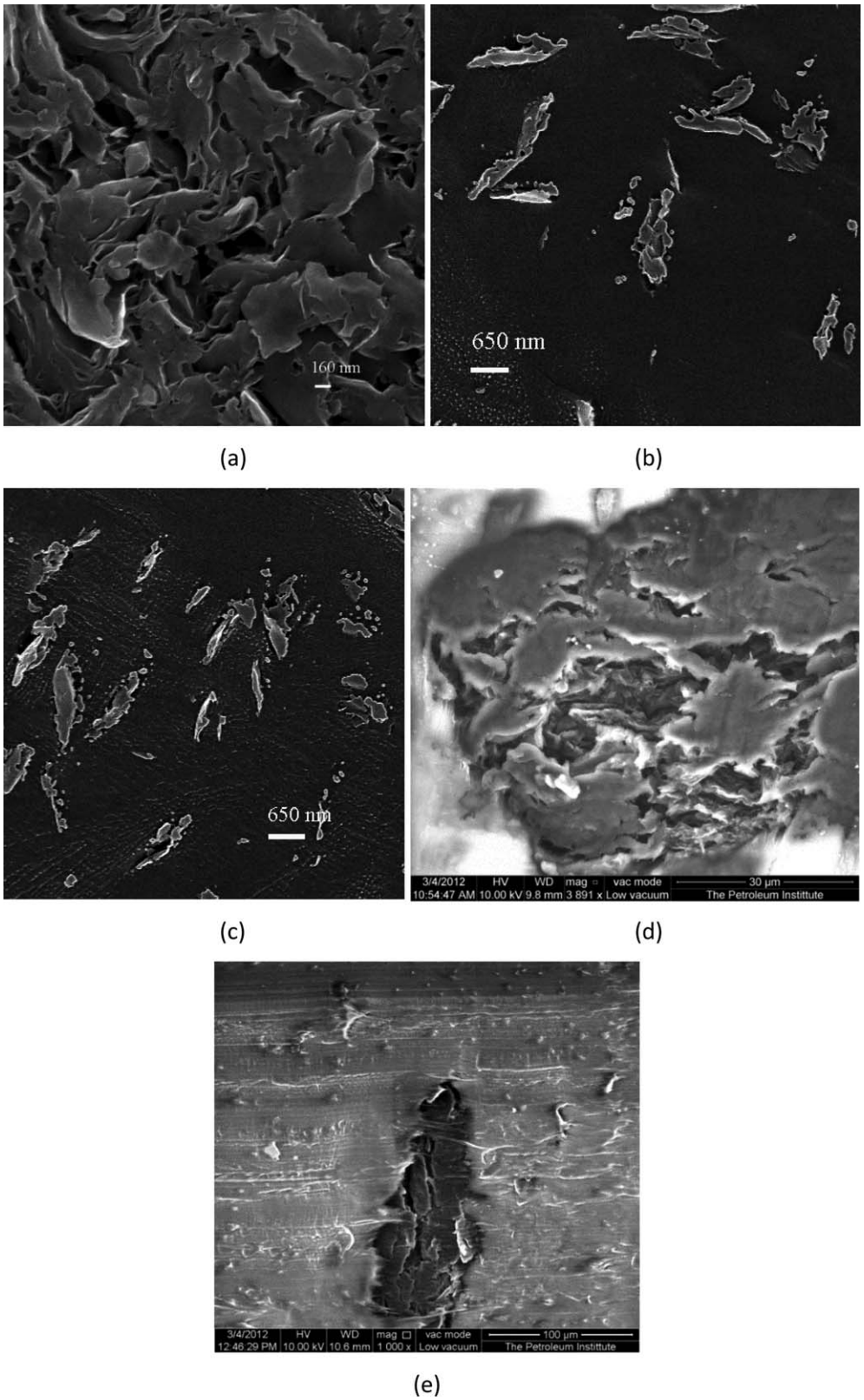

Figure 5. SEM micrographs of (a) pristine graphene; (b) PE/G/CPE25; (c) PE/G/EAA; (d) PE/G/EVA-MA; and (e) PE/G/PE-MA nanocomposites.

CPE25, EAA, EVA-MA, and PE-MA compatibilizers (cross-section of injection molded samples). The graphene platelets were observed to be bent and folded and had intertwined network which underlined the challenge in achieving their nanoscale dispersion in the polymer matrices in the short compounding periods. EAA and CPE25 containing nanocomposites exhibited

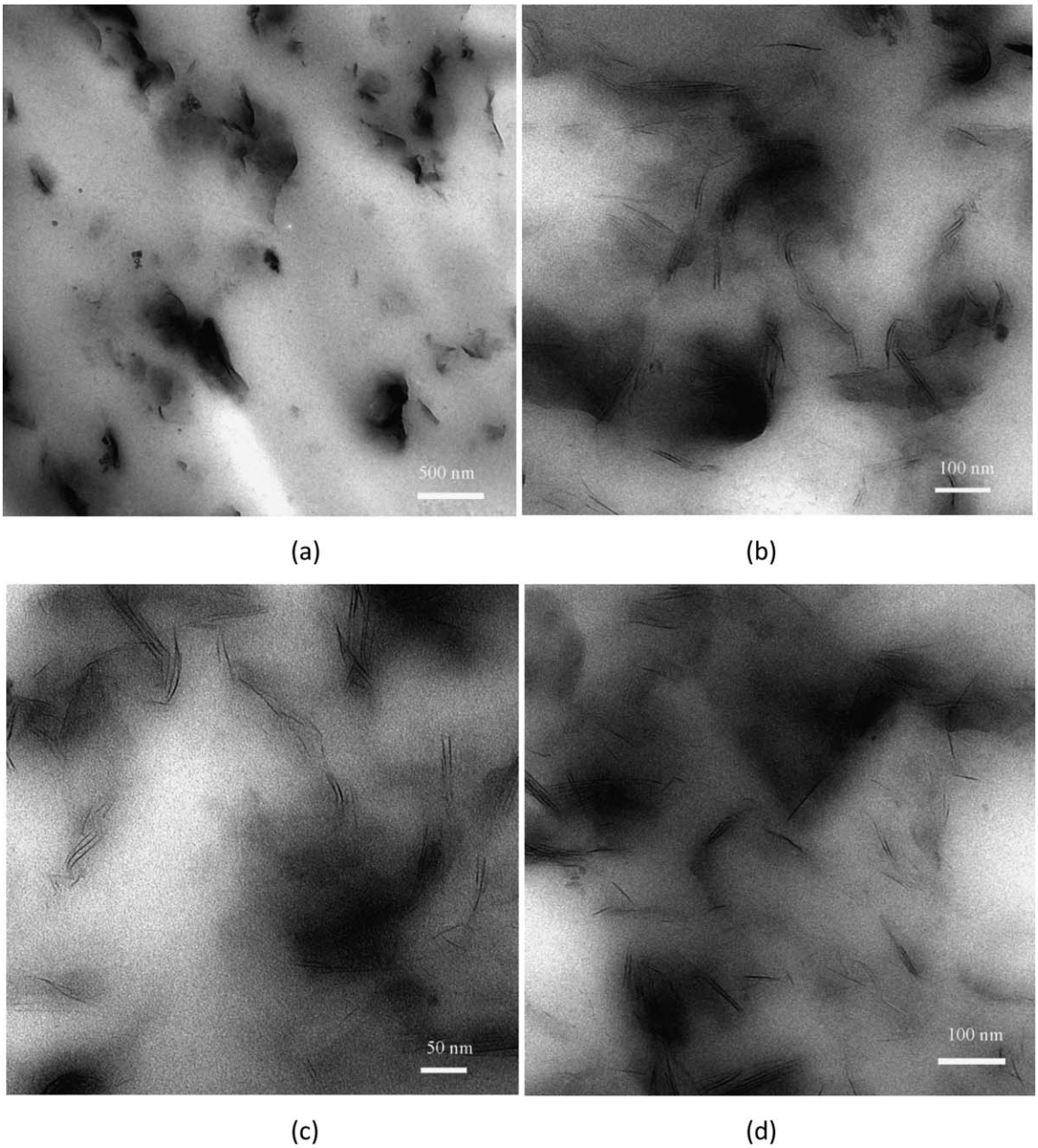

Figure 6. TEM micrographs of (a) and (b) PE/G/5% EAA nanocomposite at different magnifications; (c) PE/G/10% EAA nanocomposite; and (d) PE/G/15% EAA nanocomposite.

uniform distribution of filler and lower stack thicknesses, which also indicated that the shear experienced during compounding was sufficient to cause the filler delamination. The composites with EVA-MA and PE-MA compatibilizers had the presence of very large filler aggregates and poor interfacial adhesion. The other compatibilizers had mostly intercalated morphology in which filler stacks of varying thicknesses were observed in the polymer matrix. CPE25 in an earlier study[23] was reported to chemically interact with the graphene surface by forming ester bonds during compounding at high temperature. EAA, on the other hand, did not show any significant chemical interaction in infra-red (IR) region with the graphene platelets. Thus, the observed enhancements in the properties in this case were due to physical interactions like hydrogen bonding between the two phases leading to better filler exfoliation. The distribution of comaptibilizer in the composite should also be further studied in order to confirm its interactions with the filler surface. Though it is beneficial to have a good interaction between the compatibilizer and the filler phases, but accumulation of compatibilizer near the filler surface may also cause compatibility concerns with the matrix polymer, thus a balance in these phenomena is required.

The mechanical, rheological, thermal, and morphological analysis of the composites revealed that both EAA and CPE25 were

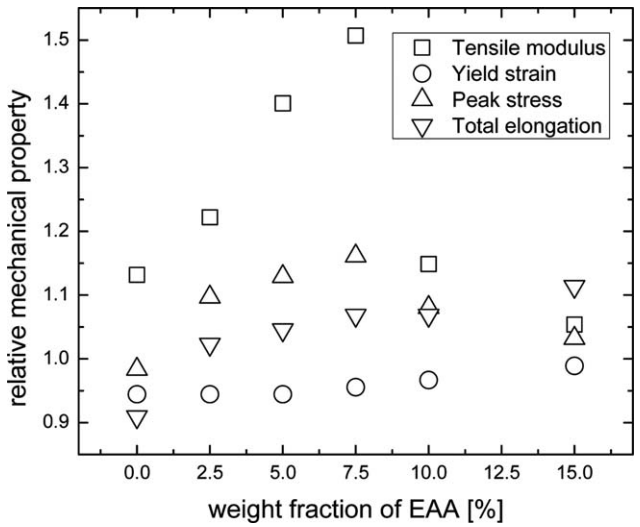

Figure 7. Relative mechanical properties of nanocomposites generated by varying amounts of EAA compatibilizer (filler content: 1 wt %).

effective compatibilizers to generate nanocomposites. Though enhancement in modulus was higher in the case of CPE25, but it also resulted in relatively higher reduction in yield strain and overall elongation as compared to EAA. In addition, EAA also resulted in maximum increase in storage modulus as well as thermal stability of the composite due to extensive exfoliation of the filler.

Based on the observed effects of filler exfoliation and corresponding enhancements in the nanocomposite properties, a series of nanocomposites with varying extents of EAA were further generated to obtain an optimum amount of EAA for property enhancement. Figure 6 shows the TEM images of the PE/G/EAA nanocomposites with 5, 10, and 15 wt % EAA content. The filler was observed to be extensively exfoliated in the composites confirming positive interactions between the filler and compatibilizer. In composite with 5% EAA content, a number of single graphene platelets were observed and the average stack thickness was also low (~4–5). No specific alignment of fillers in any particular flow or processing directions was observed (Figure 6a). The platelets were also observed to be occasionally bent and folded. Increasing the EAA content in the nanocomposites enhanced the extent of filler exfoliation and more single layers as well as graphene stacks with lower thickness were observed (Figures 6c and 6d).

Figure 7 shows the mechanical properties of nanocomposites with EAA content from 0 till 15 wt %. The tensile modulus exhibited a gradual improvement till 7.5 wt % EAA content and an increase of 50% as compared to pure PE was observed. Thus, as the compatibilizer content was enhanced, higher extent of observed filler exfoliation also resulted in enhanced mechanical performance. As the EAA content was further increased, the tensile modulus decreased significantly due to extensive matrix plasticization. At 15% EAA content, the modulus of the nanocomposites reduced to 1120 MPa. This confirmed that the filler exfoliation effect dominated the mechanical performance till 7.5 wt % content, but beyond this amount the matrix plasticization effect became dominant even though filler exfoliation increased on enhancing EAA content. However, it should also be noted that PE-EAA matrix with different amounts of EAA content had lower tensile modulus than the pure PE. Thus, the increased modulus on the addition of EAA and graphene, as observed above, is even higher in magnitude when compared to actual PE-EAA matrix, instead of pure PE. Similar to the tensile modulus, the peak stress in the nanocomposites increased till 7.5 wt % EAA content and decreased thereafter. The yield strain as well as total elongation in the nanocomposites increased as a function of EAA content due to the plasticization of the matrix by the addition of low molecular weight compatibilizer. Comparing the performance with the other filler systems, the polypropylene nanocomposites were observed to have an increment of 26% at 3 vol % (6 wt %) of polypropylene-g-maleic anhydride and 6 wt % surface-modified clay,[31] which confirmed the potential of thermally reduced graphene as reinforcing filler in

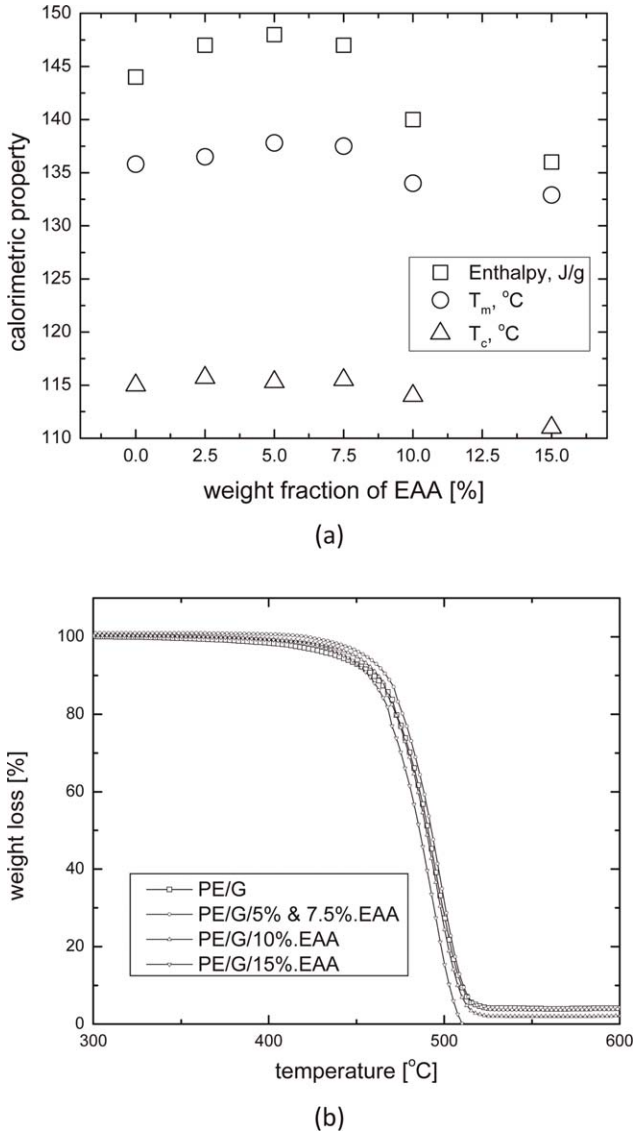

Figure 8. (a) DSC and (b) TGA thermograms of nanocomposites generated as a function of EAA compatibilizer content in the composites.

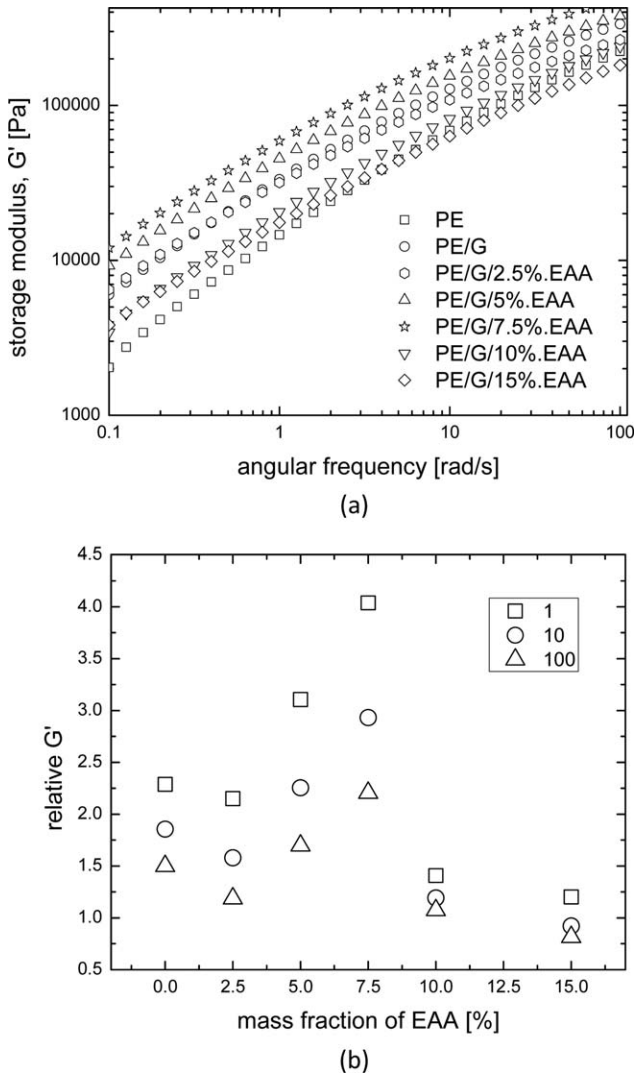

Figure 9. (a) Storage modulus of nanocomposites as a function of angular frequency and EAA content and (b) relative increase in the storage modulus of nanocomposites at angular frequencies of 1, 10, and 100 rad/s.

nanocomposites. Similarly, polyethylene nanocomposites compatibilized with 7 wt % of polyethylene-block–polyethylene glycol copolymer had an increment of 60% in tensile modulus, but the improvement was attained by using 2.8 vol % (~6 wt %) of surface-modified clay.[21] In both the cases, the stress at break in the nanocomposites decreased as compared to pure polymer, which, on the other hand, was increased with graphene as filler.

Figure 8a shows the calorimetric behavior of nanocomposites as a function of EAA content. The melt enthalpy of the polymer was observed to reach a plateau around 2.5 wt % EAA content and did not show any significant change on increasing the EAA content till 7.5 wt %. At higher EAA content, the melt enthalpy decreased significantly due to hindrance by the large amount of EAA to polymer crystallization. These findings also confirmed the observations made for tensile properties. Similarly, the peak melting point also exhibited a slight increase till 5 wt % EAA and reached a plateau. Beyond 7.5 wt %, there was a decrease in the melting point due to reduced crystallinity. The peak crystallization temperature remained unchanged till 7.5 wt %, but showed similar decrease in further enhancing the amount of EAA in the nanocomposites. The DSC thermograms also had single transition till 10 wt %, indicating compatibility. The composite with 15% EAA content exhibited a small shoulder in the DSC thermogram as the large amount of EAA would have resulted in incompatibility with the matrix polymer. These results confirmed that the properties of the nanocomposites were enhanced till 7.5 wt % of EAA, beyond which a significant reduction was observed due to matrix plasticization. Though higher extent of EAA resulted in the higher extent of filler exfoliation, a significantly higher amount of EAA in the PE matrix negated the positive impact of filler exfoliation. Similar phenomenon has also been observed for polypropylene–clay nanocomposites compatibilized with graft copolymer polypropylene-g-maleic anhydride.[31] The thermal degradation behavior of the nanocomposites is also compared in Figure 8b. The composite with 5% EAA content had better thermal stability than the PE/G nanocomposite. The curve for composite with 7.5 wt % exactly overlapped with the 5% EAA composite. The nanocomposites generated with further increased amounts of EAA exhibited slightly reduced thermal stability than the PE/G nanocomposites. However, the thermal performance was still satisfactory for their high temperature processing and applications.

Figure 9 demonstrates the rheological performance of the nanocomposites with varying extents of EAA compatibilizer. Similar to tensile modulus, the storage modulus (Figure 9a) enhanced till 7.5 wt %, but subsequently decreased with further enhancing the EAA content. At lower frequencies, the composite with 2.5 wt % EAA had similar storage modulus as PE/G composite, whereas the composite with 15% EAA content had storage modulus even lower than the pure polymer at higher frequencies. The transition frequency between G′ and G″ was also shifted to higher frequencies in composites with 10% and 15% EAA, indicating increased dominance of viscous behavior. Figure 9b also shows the relative increase in storage modulus as a function of mass fraction of EAA in the nanocomposites at 1, 10, and 100 rad/s angular frequencies. As observed in Figure 9a, the modulus increased for all three frequencies till 7.5 wt % EAA in the composites with maximum extent of improvement observed for 1 rad/s. The modulus increased more than 4 times at 1 rad/s for the PE/G/7.5%EAA nanocomposite at 1 rad/s, whereas the enhancement was 3 and 2.25 times for 10 and 100 rad/s, respectively. On increasing the comaptibilizer content beyond 7.5 wt %, the storage modulus decreased significantly and the relative differences in the magnitude of storage modulus at different angular frequencies also diminished. The viscosity of the nanocomposites also exhibited the similar behavior as the shear modulus, indicating that the 7.5 wt % content of EAA in the nanocomposites was the optimum amount to achieve enhancement in properties.

Comparing the study with the literature, it can be mentioned that a large variety of copolymers were explored in the current study for their effect on the properties of the composites. The results could be analyzed on the basis of the chemical architectures, co-monomer content, density, melting point, etc., of the compatibilizers. In one of the reported study on PE-graphene (C/O ratio of ~13) nanocomposites,[26] the authors mentioned that the tensile properties of the composites were too poor to

carry out the tensile test. Probably, the composites generated by compounding PE copolymers with graphene in the literature study were useful as masterbatches. On the other hand, the current study demonstrated generation of bulk nanocomposites and the whole spectrum of mechanical, thermal, and morphological proprieties have been characterized.

CONCLUSIONS

Role of compatibilizers of different specifications and functionalities on the microstructure and properties of polyethylene–graphene nanocomposites was studied in the current study. Addition of compatibilizers enhanced the mechanical properties of the nanocomposites and an increment of 40–45% in tensile modulus was observed for nanocomposites with CPE25, E-AO, and EAA compatibilizers. The molecular weight, extent of grafting, and polarity in the compatibilizers were the factors which determined their interactions with the filler surface. The rheological and thermal degradation properties also followed the trends observed for tensile properties. To attain an optimum amount of compatibilizer in the nanocomposites for property enhancement, the amount of best performing comaptibilizer EAA was varied in the composites. The observed properties from these composites revealed that 7.5 wt % was the optimum amount of EAA in the composites as the mechanical and rheological properties exhibited improvement due to filler exfoliation. Beyond 7.5 wt % content of EAA in the composites, the extent of filler exfoliation though was observed to increase, the performance of the nanocomposites deteriorated due to matrix plasticization. Thus, the observed behavior in the nanocomposites was a combined result of competing factors like filler exfoliation and matrix plasticization. The generated nanocomposites also exhibited much better performance as compared to the composites with commonly used clay minerals.

REFERENCES

1. Mukhopadhyay, P.; Gupta, R. K. *Plast. Eng.* **2011**, *67*, 32.
2. Kim, H.; Abdala, A. A.; Macosko, C. W. *Macromolecules* **2010**, *43*, 6515.
3. Cai, D.; Song, M. *J. Mater. Chem.* **2010**, *20*, 7906.
4. Rafiee, M. A.; Rafiee, J.; Wang, Z.; Song, H.; Yu, Z. Z.; Koratkar, N. *ACS Nano* **2009**, *3*, 3884.
5. Steurer, P.; Wissert, R.; Thomann, R.; Muelhaupt, R. *Macromol. Rapid Commun.* **2009**, *30*, 316.
6. Kim, H.; Miura, Y.; Macosko, C. W. *Chem. Mater.* **2010**, *22*, 3441.
7. Nguyen, D. A.; Lee, Y. R.; Raghu, A. V.; Jeong, H. M.; Shin, C. M.; Kim, B. K. *Polym. Int.* **2009**, *58*, 412.
8. Fang, M.; Wang, K.; Lu, H.; Yang, Y.; Nutt, S. *J. Mater. Chem.* **2009**, *19*, 7098.
9. Potts, J. R.; Dreyer, D. R.; Bielawski, C. W.; Ruoff, R. S. *Polymer* **2011**, *52*, 5.
10. Liu, H.; Brinson, L. C. *Compos. Sci. Technol.* **2008**, *68*, 1502.
11. Reddy, B. Advances in Diverse Industrial Applications of Nanocomposites; InTech: Rijeka, **2011**.
12. Hui, L.; Smith, R. C.; Wang, X.; Nelson, J. K.; Schadler, L. S. *Conf. Electr. Insul. Dielectr. Phenomena* **2008**, *317*.
13. Manas-Zloczower, I. *Rheol. Bull.* **1997**, *66*, 5.
14. Lee, S. H.; Cho, E.; Jeon, S. H.; Youn, J. R. *Carbon* **2007**, *45*, 2810.
15. Serageldin, M. A.; Wang, H. *Thermochim. Acta* **1987**, *117*, 157.
16. Ramanathan, T.; Abdala, A. A.; Stankovich, S.; Dikin, D. A.; Herrera-Alonso, M.; Piner, R. D.; Adamson, D. H.; Schniepp, H. C.; Chen, X.; Ruoff, R. S.; Nguyen, S. T.; Aksay, I. A.; Prud'Homme, R. K.; Brinson, L. C. *Nat. Nanotechnol.* **2008**, *3*, 327.
17. Ansari, S.; Giannelis, E. P. *J. Polym. Sci. Part B* **2009**, *47*, 888.
18. Castelain, M.; Martinez, G.; Marco, C.; Ellis, G.; Salavagione, H. J. *Macromolecules* **2013**, *46*, 8980.
19. Wang, J.; Xu, C.; Hu, H.; Wan, L.; Chen, R.; Zheng, H.; Liu, F.; Zhang, M.; Shang, X.; Wang, X. *J. Nanopart. Res.* **2011**, *13*, 869.
20. Yun, Y. S.; Bae, Y. H.; Kim, D. H.; Lee, J. Y.; Chin, I. J.; Jin, H. J. *Carbon* **2011**, *49*, 3553.
21. Osman, M. A.; Rupp, J. E. P.; Suter, U. W. *Polymer* **2005**, *46*, 8202.
22. Schniepp, H. C.; Li, J.-L.; McAllister, M. J.; Sai, H.; Herrera-Alonso, M.; Adamson, D. H.; Prud'homme, R. K.; Car, R.; Saville, D. A.; Aksay,I. A. *J. Phys. Chem. B* **2006**, *110*, 8535.
23. Chaudhry, A. U.; Mittal, V. *Polym. Eng. Sci.* **2013**, *53*, 78.
24. Vasileiou, A. A.; Kontopoulou, M.; Docoslis, A. *ACS Appl. Mater. Interfaces* **2014**, *6*, 1916.
25. Yu, B.; Wang, X.; Qian, X.; Xing, W.; Yang, H.; Ma, L.; Lin, Y.; Jiang, S.; Song, L.; Hu, Y.; Lo, S. *RSC Adv.* **2014**, *4*, 31782.
26. Seo, H. M.; Park, J. H.; Dao, T. D.; Jeong, H. M. *J. Nanomater.* **2013**, 805201.
27. McAllister, M. J.; Li, J. L.; Adamson, D. H.; Schniepp, H. C.; Abdala, A. A.; Liu, J.; Herrera-Alonso, M.; Milius, D. L.; Car, R.; Prud'homme, R. K.; Aksay, I. A. *Chem. Mater.* **2007**, *19*, 4396.
28. Hummers, W. S.; Offeman, R. E. *J. Am. Chem. Soc.* **1958**, *80*, 1339.
29. Joshi, M.; Butola, B. S.; Simon, G.; Kukaleva, N. *Macromolecules* **2006**, *39*, 1839.
30. Mittal, V.; Chaudhry, A. U.; Matsko, N. B. *J. Appl. Polym. Sci.* **2014**, *131*, 40816.
31. Mittal, V. *J. Appl. Polym. Sci.* **2008**, *107*, 1350.